

Artifacts in incomplete data tomography with applications to photoacoustic tomography and sonar

Jürgen Friel^{*}

Eric Todd Quinto[†]

Abstract

We develop a paradigm using microlocal analysis that allows one to characterize the visible and added singularities in a broad range of incomplete data tomography problems. We give precise characterizations for photo- and thermoacoustic tomography and Sonar, and provide artifact reduction strategies. In particular, our theorems show that it is better to arrange Sonar detectors so that the boundary of the set of detectors does not have corners and is smooth. To illustrate our results, we provide reconstructions from synthetic spherical mean data as well as from experimental photoacoustic data.

1 Introduction

In many types of computed tomography, such as x-ray tomography, photoacoustic (and thermoacoustic) tomography (PAT/TAT) or Sonar, the tomographic projections can be acquired only from a limited field of view. As a result, the data are highly incomplete and the corresponding reconstruction problem becomes severely ill-posed which leads to serious instabilities of the reconstruction process. As a consequence two phenomena can be observed in practical reconstructions: First, only specific features of the unknown object (visible singularities) can be reconstructed reliably, cf. [28, 33] and Figure 1. Second, and even more important, additional singularities (artifacts) can be generated during the reconstruction and superimpose reliable information, cf. [11, 19] and Figure 1. This is a serious problem, since artifacts can overlap and generate new image features leading to misinterpretations or possibly misdiagnosis in medical imaging applications. It is therefore essential to develop a precise understanding of such artifacts for a range of imaging situations and to provide algorithms that reliably reconstruct the information that is contained in the data and at the same time avoid the generation of unwanted features.

The generation of artifacts in incomplete data PAT and Sonar has been addressed in several publications, eg. [4, 14, 18, 23, 24, 30, 39], to mention only a few. In particular, it has been observed that those artifacts occur due to hard truncation of the data. In order to reduce the generation of artifacts in practical reconstructions, some authors therefore use smooth truncation of the limited view data. Although it is intuitively understood why artifacts occur and how to deal with them, to the best of our knowledge, no theoretical (geometrical) characterization of artifacts was given so far - neither in PAT nor in Sonar. Also, it has not yet been mathematically justified, in general, why smooth truncation reduces artifacts (see Remark A.2).

In this article, we use the framework of microlocal analysis and the calculus of Fourier integral operators to develop a general approach that enables one to mathematically characterize limited angle artifacts for different types of tomography problems. We show that the reason for artifact generation is the hard truncation of the data at the ends of the angular range, and that they can be reduced by using a smooth truncation. We provide a paradigm that applies to a broad range of limited data problems and derive explicit characterizations of artifacts PAT/TAT and Sonar. Moreover, we illustrate our results in numerical experiments on simulated and experimental PAT data.

^{*}Department of Mathematics, Tufts University, Medford, MA 02155, USA and Institute of Computational Biology, Helmholtz Zentrum München, Germany, **Email:** juergen.friel@helmholtz-muenchen.de

[†]Department of Mathematics, Tufts University, Medford, MA 02155, USA; **Email:** todd.quinto@tufts.edu

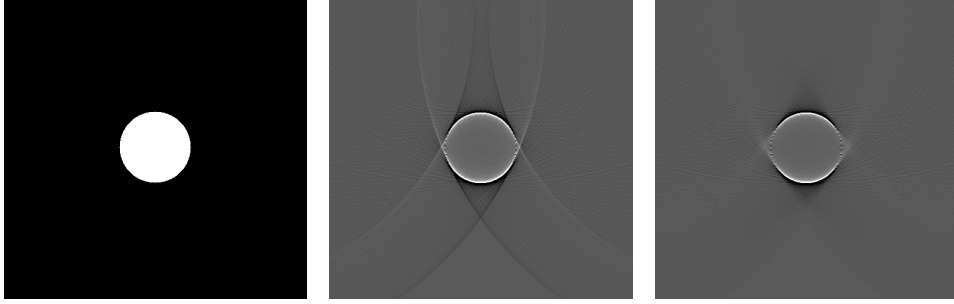


Figure 1: Lambda type reconstruction from limited view spherical mean data for the limited angular range $[25^\circ, 155^\circ]$ (361 projections, 725 radii). *Left*: original image (512×512 , characteristic function of a disc centered at the origin); *Middle*: Lambda reconstruction without artifact reduction; *Right*: Lambda reconstruction with artifact reduction.

Characterizations of limited angle artifacts for x-ray tomography were obtained in [19] and [11], where also a smooth truncation of the limited data was proposed to reduce the artifacts. Katsevich's results [19] apply to the line transform with arbitrary smooth weights. The results in [11, 19] have been derived in a way which does not directly generalize to other tomography problems. This is mainly due to the fact that the authors heavily rely on the explicit expression of the reconstruction operators as singular pseudodifferential operators. However, for many other tomography problems such formulas are not available and, hence, the techniques of [11, 19] cannot be applied in order to get similar characterizations. Nguyen has qualitatively analyzed the strength of the added artifacts occurring in limited angle tomography [25]. His recent article [26] uses ideas from this article plus microlocal, asymptotic arguments to calculate the strength of the artifacts for the spherical transform in cases related to the ones we discuss here. In [29] microlocal analysis is used to understand the streaks in X-ray CT scans caused by metal. In [37], Symes observed the advantages of soft truncation (p. 46-47) and the problems with hard truncation (p. 65) in seismic imaging.

This article is organized as follows. In Section 2 we introduce the basic microlocal analysis needed for the article, including fundamental theorems about Fourier integral operators. Then, in Section 3, we give the key Theorem 3.1, describe the general strategy, and outline our paradigm to characterize the added singularities. This will guide the proofs and show how the paradigm can be used in general. In Section 4, we apply these results to thermo- and photoacoustic tomography and Sonar. In section 5 we provide reconstructions from real data to show how the artifacts occur and how they can be decreased. Finally, in section 6, we make some general observations about our method. Proofs of our main theorems are provided in the Appendix.

2 Microlocal Analysis and Fourier Integral Operators

In this section we review basic facts from microlocal analysis and the calculus of Fourier integral operators (including fundamental theorems) needed for the article. For general facts about the theory of distributions and more details on microlocal analysis we refer to [10, 17]. For details on Fourier integral operators we refer to [16, 38].

Let Ω be an open set. We denote the set of C^∞ functions with domain Ω , by $\mathcal{E}(\Omega)$ and the set of C^∞ functions of compact support in Ω by $\mathcal{D}(\Omega)$. Distributions are continuous linear functionals on these function spaces. The dual space to $\mathcal{D}(\Omega)$ is denoted $\mathcal{D}'(\Omega)$ and the dual space to $\mathcal{E}(\Omega)$ is denoted $\mathcal{E}'(\Omega)$. In fact, $\mathcal{E}'(\Omega)$ is the set of distributions of compact support in Ω . For more information about these spaces we refer to [36].

A function $f(\xi)$ is said to *decay rapidly at infinity in a conic open set V* if it decays faster than any power of $1/\|\xi\|$ in V . The singular support of a distribution, f , $\text{sing supp}(f)$, is the complement of the largest open set on which f is a C^∞ function. It follows directly from this definition that $\text{sing supp}(f) \subset \text{supp}(f)$, and $\text{sing supp}(f) = \emptyset$ if and only if $f \in C^\infty(\mathbb{R}^n)$.

To make the concept of singularity apply to our range of problems, we will need to view the wavefront³ set as a subset of a conormal bundle so it will be invariantly defined on manifolds [38]. If Ξ is a manifold and $y \in \Xi$, then the cotangent space of Ξ at y is the set of all first order differentials (the dual space to the tangent space $T_y(\Xi)$), and the cotangent bundle $T^*(\Xi)$ is the vector bundle with fiber above $y \in \Xi$. That is $T^*(\Xi) = \{(y, \eta) : y \in \Xi, \eta \in T_y^*(\Xi)\}$.

For example, the differentials $\mathbf{dx}_1, \mathbf{dx}_2, \dots$, and \mathbf{dx}_n are a basis of $T_x^*(\mathbb{R}^n)$ for any $x \in \mathbb{R}^n$. For $\xi \in \mathbb{R}^n$, we will use the notation

$$\xi \mathbf{dx} = \xi_1 \mathbf{dx}_1 + \xi_2 \mathbf{dx}_2 + \dots + \xi_n \mathbf{dx}_n \in T_x^*(\mathbb{R}^n).$$

If $\phi \in \mathbb{R}$ then $\mathbf{d}\phi$ will be the differential with respect to ϕ and \mathbf{dr} and \mathbf{ds} are defined analogously.

If ϕ is a function of x, y then $\mathbf{d}_x\phi$ is the differential of ϕ in x , so if $\nabla_x\phi$ is the gradient of ϕ in x , then

$$\mathbf{d}_x\phi = \nabla_x\phi \mathbf{dx}. \quad (1)$$

The differentials of ϕ in other variables will be defined in a similar way.

Definition 2.1 (Wavefront Set [17]). Let $f \in \mathcal{D}'(\mathbb{R}^n)$, $x_0 \in \mathbb{R}^n$ and $\xi_0 \in \mathbb{R}^n \setminus \mathbf{0}$. Then f is *microlocally smooth at x_0 in direction ξ_0* if there is a cutoff function φ (a smooth function of compact support for which $\varphi(x_0) \neq 0$) and a conic neighborhood of ξ_0 such that the localized Fourier transform $(\widehat{\varphi f})$ is rapidly decreasing at infinity in V .

The *wavefront set* of f is the set $\text{WF}(f)$ of all $(x, \xi \mathbf{dx}) \in T^*(\mathbb{R}^n) \setminus \mathbf{0}$ such that f is *not* microlocally smooth at x in direction ξ .

Example 2.1. Let K be a compact subset of \mathbb{R}^2 bounded by a simple closed smooth curve $B = \text{bd}(\Omega)$. Then, the wavefront set of the characteristic function of K , χ_K , is the set of covectors conormal to the boundary of K :

$$(y, \eta \mathbf{dy}) \in \text{WF}(\chi_K) \quad \Leftrightarrow \quad y \in \text{bd}(K), \eta \in N_y, \quad (2)$$

where N_y is the set of all vectors normal to $\text{bd}(K)$ at y . The proof of this fact is non-trivial. The wavefront set of the characteristic function of a square is the set of conormals to the sides plus all covectors above the corners of the square (see [31, Example 9.12, p. 219]). This can be used to show (2) by using the Inverse Function Theorem to find a diffeomorphism to locally straighten out the boundary curve. Then note that the diffeomorphism takes conormals to one boundary (i.e., wavefront set) to conormals of the other.

However, if $\text{bd}(K)$ is piecewise smooth and has a corner at a point y then all covectors above y are in $\text{WF}(\chi_K)$. This follows from the same example in [31] or a Radon line transform argument.

We now introduce Fourier Integral Operators (FIO) and provide some of their properties. These operators are generalizations of differential operators and they alter wavefront sets in precise ways.

Definition 2.2 ([38]). Let $Y \subset \mathbb{R}^m$ and $X \subset \mathbb{R}^n$ be open subsets. A real valued function $\phi \in C^\infty(Y \times X \times \mathbb{R}^N \setminus \{0\})$ is called a *phase function* if

1. ϕ is positive-homogeneous of degree 1 in ξ . That is $\phi(y, x, r\xi) = r\phi(y, x, \xi)$ for all $r > 0$.
2. $(\mathbf{d}_y\phi, \mathbf{d}_\xi\phi)$ and $(\mathbf{d}_x\phi, \mathbf{d}_\xi\phi)$ do not vanish for all $(y, x, \xi) \in Y \times X \times \mathbb{R}^N \setminus \{0\}$ where \mathbf{d}_x is defined in (1) and the other operators are defined in a similar way.

We define the auxiliary manifold

$$\Sigma_\phi = \{(y, x, \xi) \in Y \times X \times (\mathbb{R}^N \setminus \mathbf{0}) : \mathbf{d}_\xi\phi(y, x, \xi) = 0\}. \quad (3)$$

The phase function ϕ is called non-degenerate if the set $\{\mathbf{d}_{y,x,\xi} \left(\frac{\partial \phi}{\partial \xi_j} \right), 1 \leq j \leq N\}$ is linearly independent on Σ_ϕ .

Definition 2.3 ([38]). A Fourier integral operator (FIO) \mathcal{F} is defined as

4

$$\mathcal{F}u(y) = \int e^{i\phi(y,x,\xi)} p(y,x,\xi) u(x) dx d\xi,$$

where ϕ is a non-degenerate phase function, and the amplitude $p(y,x,\xi) \in C^\infty(Y \times X \times \mathbb{R}^n)$ satisfies the following estimate: For every compact set $K \subset Y \times X$ and for every multi-index α, β, γ , there is a constant $C = C(K, \alpha, \beta, \gamma)$ such that

$$|D_\xi^\alpha D_x^\beta D_y^\gamma p(y,x,\xi)| \leq C(1 + \|\xi\|)^{m-|\alpha|} \text{ for all } x, y \in K \text{ and for all } \xi \in \mathbb{R}^n.$$

The *canonical relation* of \mathcal{F} is defined as

$$C := \{(y, \mathbf{d}_y \phi(y, x, \xi); x, -\mathbf{d}_x \phi(y, x, \xi)) : (y, x, \xi) \in \Sigma_\phi\}. \quad (4)$$

Note that since the phase function ϕ is non-degenerate, the sets Σ_ϕ and C are smooth manifolds. Furthermore, C is conic in the cotangent variables

To understand what Fourier integral operators and their compositions do on wavefront sets, we will define compositions of canonical relations. Let X and Y be manifolds, and $A \subset T^*(X) \times T^*(Y)$, then

$$\begin{aligned} A' &= \{(x, \xi; y, -\eta) : (x, \xi; y, \eta) \in A\}, \\ A^t &= \{(y, \eta; x, \xi) : (x, \xi; y, \eta) \in A\}. \end{aligned} \quad (5)$$

If $B \subset T^*(Y) \times T^*(X)$ and $C \subset T^*(X)$, we define

$$B \circ C = \{(y, \eta) \in T^*(Y) : \exists (x, \xi) \in C : (y, \eta; x, \xi) \in B\},$$

and

$$\begin{aligned} A \circ B &= \{(x, \xi; x', \xi') \in T^*(X) \times T^*(X) : \\ &\quad \exists (y, \eta) \in T^*(Y) : (x, \xi; y, \eta) \in A \text{ and } (y, \eta; x', \xi') \in B\}. \end{aligned} \quad (6)$$

For later use, we note the following relations: For A, B , and C as above and $\tilde{C} \subset T^*(X)$

$$B \circ (C \cup \tilde{C}) = (B \circ C) \cup (B \circ \tilde{C}), \quad A \circ (B \circ C) = (A \circ B) \circ C. \quad (7)$$

Note that a linear operator, $L : \mathcal{E}'(X) \rightarrow \mathcal{D}'(Y)$ is *properly supported* when the following holds: if S is the support of the Schwartz kernel of L , then the projections from S to X and to Y are compact maps (i.e., the inverse image of any compact set is compact). This implies that $L : \mathcal{E}'(X) \rightarrow \mathcal{E}'(Y)$. Now we make use of the fact that Fourier integral operators satisfy the Hörmander Sato Lemma.

Theorem 2.4 (Th. 5.4, p. 461 [38]). *Let f be a distribution of compact support and let \mathcal{F} be a Fourier integral operator. Then,*

$$\text{WF}(\mathcal{F}f) \subset C \circ \text{WF}(f). \quad (8)$$

If \mathcal{F} is properly supported, then this inclusion is valid for any distribution.

Furthermore we have that the adjoint of a FIO is a FIO.

Theorem 2.5 (Thm. 4.2.1 p. 174 [16]). *If \mathcal{F} is an FIO associated to the canonical relation C , then the adjoint \mathcal{F}^* is an FIO associated to C^t .*

These theorems and the composition relations for FIO will be the keys to our general strategy in the next section and the proofs in the subsequent sections.

3 General Strategy

In this section, we will outline the general ideas we will apply in the following sections to understand visible and added singularities in limited data tomography. By presenting the ideas in general, we emphasize the broad applicability of this mathematics.

The imaging operator will be denoted $\mathcal{M} : \mathcal{E}'(\Omega) \rightarrow \mathcal{E}'(\Xi)$, where the *object space* Ω is a region in space to be imaged and the *data space* Ξ is a space that parameterizes the data. For the planar X-ray transform, the imaging operator is the X-ray transform, Ω is an open set in \mathbb{R}^2 containing the object to be imaged, and Ξ is the set of lines in \mathbb{R}^2 . In what follows the operator \mathcal{M} is assumed to be a FIO. In this article, we consider incomplete data problems in which the data are taken only on a closed set $A \subset \Xi$. The resulting forward operator can be written

$$\mathcal{M}_A f = \chi_A \mathcal{M}, \tag{9}$$

where χ_A is the characteristic function of A and the product just restricts the data to the set A . In the cases we consider, the reconstruction operator is of the form

$$\mathcal{M}^* P \mathcal{M}_A, \tag{10}$$

where \mathcal{M}^* is an appropriate dual or backprojection operator to \mathcal{M} that takes functions on the data space to functions on the object space and P is a differential or pseudodifferential operator. Equation (10) models many standard reconstruction algorithms, including limited angle filtered backprojection [23], Lambda tomography [7, 8], and algorithms in thermoacoustic tomography [9, 21] and sonar [3], and radar [27].

Since \mathcal{M} is assumed to be a FIO, Theorem 2.4 and the wavefront relation (8) tells what \mathcal{M} and \mathcal{M}^* do to $\text{WF}(f)$. Our next theorem tells what multiplication by χ_A does to the wavefront set. It is a special case of Theorem 8.2.10 in [17].

Theorem 3.1. *Let $u \in \mathcal{D}'(\Xi)$, and let A be a closed subset of Ξ with nontrivial interior. If the non-cancellation condition*

$$\forall (y, \xi) \in \text{WF}(u), (y, -\xi) \notin \text{WF}(\chi_A) \tag{11}$$

holds, then the product $\chi_A u$ can be defined as a distribution. In this case, we have

$$\text{WF}(\chi_A u) \subset \mathcal{Q}(A, \text{WF}(u)), \tag{12}$$

where, for $W \subset T^(\Xi)$,*

$$\mathcal{Q}(A, W) := \{(y, \xi + \eta) : y \in A, [(y, \xi) \in W \text{ or } \xi = 0] \text{ and } [(y, \eta) \in \text{WF}(\chi_A) \text{ or } \eta = 0]\}. \tag{13}$$

Note that the condition “ $y \in A$ ” is not in (13) in Hörmander’s theorem, but we can include this condition because $\chi_A u$ is zero (hence smooth) off of the closed set A .

An auxiliary lemma will make the paradigm easier to apply.

Lemma 3.2. *Let $\mathcal{M} : \mathcal{E}'(X) \rightarrow \mathcal{D}'(\Xi)$ be a FIO with canonical relation C and let A be a closed subset of Ξ . Assume the non-cancellation condition (11) holds for \mathcal{M} and χ_A so the Schwartz kernel of $\mathcal{M}_A = \chi_A \mathcal{M}$ is a distribution. Assume the linear operator $\mathcal{M}_A : \mathcal{E}'(X) \rightarrow \mathcal{E}'(\Xi)$ (i.e., for each $f \in \mathcal{E}'(X)$, the distribution $\mathcal{M}_A(f)$ has compact support). Let P be a properly supported pseudodifferential operator (or $\mathcal{M}^* : \mathcal{D}'(\Xi) \rightarrow \mathcal{D}'(X)$). Then,*

$$\text{WF}(P \mathcal{M}_A f) \subset \mathcal{Q}(A, C \circ \text{WF}(f)), \tag{14}$$

$$\text{WF}(\mathcal{M}^* P \mathcal{M}_A f) \subset C^t \circ \mathcal{Q}(A, C \circ \text{WF}(f)). \tag{15}$$

Proof. By Theorem 2.4, $\text{WF}(\mathcal{M}f) \subset C \circ \text{WF}(f)$. Then one uses Theorem 3.1 and the definition of \mathcal{Q} , (13), to infer

$$\text{WF}(\chi_A \mathcal{M}f) \subset \mathcal{Q}(A, \text{WF}(\mathcal{M}f)) \subset \mathcal{Q}(A, C \circ \text{WF}(f)).$$

We also just used the fact that when $W' \subset W \subset T^*(\Xi)$, then $\mathcal{Q}(A, W') \subset \mathcal{Q}(A, W)$. This finishes the proof of (14). Now, using Theorem 2.4 and the composition rules (7) for C^t , one proves (15) from (14). \square

Here is the outline of our paradigm; it can be used for a range of limited data problems to understand visible and added singularities.

- (a) Confirm the forward operator \mathcal{M} is a FIO and calculate its canonical relation, C .
- (b) Choose a closed limited data set $A \subset \Xi$ and calculate $\text{WF}(\chi_A)$ (see Example 2.1).
- (c) Make sure the non-cancellation condition (11) holds for χ_A and $\mathcal{M}f$. This can be done in general by making sure it holds for $(y, \eta) \in C \circ (T^*(\Omega) \setminus \mathbf{0})$ since that is the largest that $\text{WF}(\mathcal{M}f)$ can be (by Theorem 2.4 since $\text{WF}(f) \subset T^*(\Omega) \setminus \mathbf{0}$).
- (d) Then, calculate $\mathcal{Q}(A, C \circ \text{WF}(f))$.
- (e) By Lemma 3.2

$$\text{WF}(\mathcal{M}^* P \mathcal{M}_A f) \subset C^t \circ \mathcal{Q}(A, C \circ \text{WF}(f)), \quad (16)$$

so calculate $C^t \circ \mathcal{Q}(A, C \circ \text{WF}(f))$ to find possible visible singularities and added artifacts.

4 Characterization of Limited Data Artifacts in PAT/TAT and Sonar

Using the paradigm of section 3, we now describe the visible and added singularities for photo- and thermoacoustic tomography (PAT and TAT, respectively), and sonar with constant sound speed. Proofs will be given in the appendix.

The same arguments can be used to prove the theorems in [11] about limited angle tomography, even for the generalized X-ray transform in the plane with arbitrary smooth measures. The arguments in [11, 19] are more elementary and do not require the theory of FIO, but they do not apply to generalized transforms.

Remark 4.1. Although we state the theorems for the circular and spherical transforms with standard measures, our theorems are valid more generally. Theorems 4.2 and 4.4 are valid for the generalized circular mean transform with a smooth nowhere zero weight $\mu(\phi, x) dx$ in (18). Theorems 4.6 and 4.8 are valid for the generalized circular mean transform with a smooth nowhere zero weight $\mu(y, x) dx$ in (27). In fact, our theorems are valid for any FIO associated to the same canonical relation since our proofs use only the properties of the operators as FIO and their associated their canonical relations (when the operators can be composed).

4.1 Photo- and thermoacoustic tomography for planar data (circular Radon transform)

In this section, we consider the so-called circular mean Radon transform in 2D, which is a standard model for sectional imaging setups of photoacoustic tomography with constant sound speed. We refer to [6, 15, 20] for overviews of the mathematics behind PAT and TAT. The forward transform is defined by

$$\mathcal{M}f(\xi, r) = \frac{1}{2\pi} \int_{u \in S^1} f(\xi + ru) du, \quad (\xi, r) \in S \times (0, \infty), \quad (17)$$

where S is a smooth curve in \mathbb{R}^2 .

We will consider only functions and distributions on \mathbb{R}^2 that are supported inside the open unit disk $D = \{x \in \mathbb{R}^2 : \|x\| < 1\}$. We will assume the detectors are on the circle $S = S^1$, and use the parameterizations for vectors in S^1 and for circles respectively

$$\theta(\phi) = (\cos \phi, \sin \phi) \text{ for } \phi \in [0, 2\pi], \quad C(\phi, r) = \{x \in \mathbb{R}^2 : \|x - \theta(\phi)\| = r\}.$$

The tomographic data will have the following parametrization

7

$$\text{for } (\phi, r) \in \Xi := [0, 2\pi] \times (0, \infty), \quad g(\phi, r) = \mathcal{M}f(\phi, r) := \frac{1}{2\pi r} \int_{x \in C(\phi, r)} f(x) dx, \quad (18)$$

where we identify 0 and 2π or, equivalently, consider only functions and distributions on Ξ that are 2π periodic in ϕ . Note that the measure dx in this integral is the arc length measure.

Then, the dual transform to \mathcal{M} (using the standard measures on D and Ξ) is

$$\mathcal{M}^*g(x) = \int_0^{2\pi} g(\phi, \|x - \theta(\phi)\|) \frac{1}{2\pi \|x - \theta(\phi)\|} d\phi.$$

Because D is the open disk with boundary S^1 , $\mathcal{M} : \mathcal{D}(D) \rightarrow \mathcal{D}(\Xi)$ is continuous. Therefore, its adjoint, $\mathcal{M}^* : \mathcal{D}'(\Xi) \rightarrow \mathcal{D}'(D)$ is weakly continuous. Similarly, $\mathcal{M} : \mathcal{E}'(D) \rightarrow \mathcal{E}'(\Xi)$ is weakly continuous.

We will consider the limited data problem for this transform specifying circular means with centers $\theta(\phi)$ for $\phi \in [a, b]$ with $b - a < 2\pi$. We define

$$\mathcal{M}_{[a,b]}f = \chi_A \cdot \mathcal{M}f \quad \text{where } A = [a, b] \times (0, \infty). \quad (19)$$

The wavefront of χ_A is given by

$$\text{WF}(\chi_A) = \{((\phi, r), \nu d\phi) : \phi \in \{a, b\}, \nu \neq 0, r > 0\}. \quad (20)$$

Before we state the main theorem of the section, we need to define several concepts related to the microlocal analysis of the circular mean transform. For $\phi \in [0, 2\pi]$ and $x \in D$, let

$$\mathbf{n}(\phi, x) = \frac{x - \theta(\phi)}{\|x - \theta(\phi)\|}. \quad (21)$$

Then $\mathbf{n}(\phi, x)$ the outward unit normal vector at x to the circle $C(\phi, \|x - \theta(\phi)\|)$ centered at $\theta(\phi)$ and containing x .

For $A \subset [0, 2\pi]$ we define the set

$$\mathcal{V}_A := \{(x, \xi d\mathbf{x}) \in T^*(D) : \exists \phi \in A, \exists \alpha \neq 0, \xi = \alpha \mathbf{n}(\phi, x)\}. \quad (22)$$

In our next theorem, we show $\mathcal{V}_{[a,b]}$ is the set of *possible visible singularities*, i.e., those that can be imaged by $\mathcal{M}^*PM_{[a,b]}$ (singularities for $\phi \in \{a, b\}$ might be cancelled).

For $f \in \mathcal{E}'(D)$, we define the set

$$\begin{aligned} \mathcal{A}_{\{a,b\}}(f) := & \{(x, \xi d\mathbf{x}) \in T^*(D) : \exists \phi \in \{a, b\} \exists r \in (0, 2), \exists \alpha \neq 0, \\ & \exists \tilde{x} \in C(\phi, r) \cap D, (\tilde{x}, \alpha \mathbf{n}(\phi, \tilde{x}) d\mathbf{x}) \in \text{WF}(f) \\ & \text{and } x \in C(\phi, r) \cap D, \xi = \alpha \mathbf{n}(\phi, x)\}. \end{aligned} \quad (23)$$

The set $\mathcal{A}_{\{a,b\}}(f)$ will include *added artifacts* in the reconstruction operator $\mathcal{M}^*PM_{[a,b]}(f)$.

Theorem 4.2 (Visible and Added Singularities). *Let $f \in \mathcal{E}'(D)$ and let P be a pseudodifferential operator on $\mathcal{D}'(\Xi)$. Then,*

$$\text{WF}(\mathcal{M}^*PM_{[a,b]}f) \subset (\text{WF}(f) \cap \mathcal{V}_{[a,b]}) \cup \mathcal{A}_{\{a,b\}}(f). \quad (24)$$

One would expect that an inclusion $\text{WF}(f) \cap \mathcal{V}_{[a,b]} \subset \text{WF}(\mathcal{M}^*PM_{[a,b]}f)$ holds, which is true for sonar, as proven in Section 4.2, and for limited angle x-ray tomography with reconstruction operators considered in [11]. We will discuss why this is not possible, in general, for the PAT transform in Remark A.1.

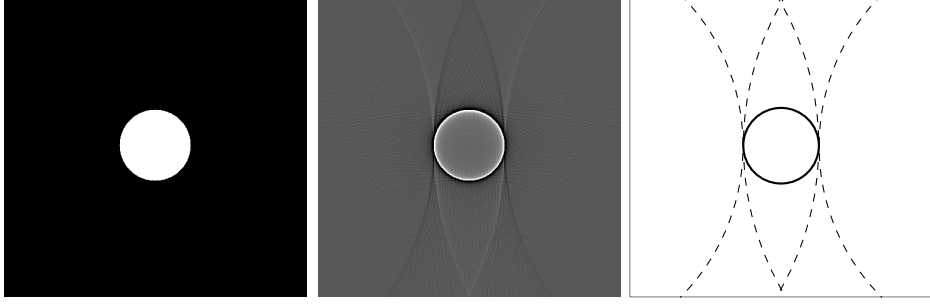


Figure 2: Lambda type reconstruction (middle) of the characteristic function of a circle (left) for the angular range $[0, \pi]$ and visualization of the set of added artifacts $\mathcal{A}_{\{0, \pi\}}$ (right). The correspondence between practical reconstruction and theoretical description (23) is remarkable.

Remark 4.3. In general, Radon transforms detect singularities conormal to the set being integrated over, and so the visible singularities should be conormal to circles in the data set. The set $\mathcal{V}_{[a, b]}$ is the collection of conormals to circles $C(\phi, r)$ for $\phi \in [a, b]$, and, according to Theorem 4.2, $\mathcal{V}_{[a, b]} \cap \text{WF}(f)$ is the set of possible visible singularities in $\mathcal{M}^*P\mathcal{M}_{[a, b]}f$. This idea of visible singularities being (co)normal to the manifold of integration is well-known and is for example, discussed in [28, 33]. This follows from the pioneering work of Guillemin [12, 13] showing Radon transforms are FIO associated to a conormal bundle.

There are also possible added singularities, $\mathcal{A}_{\{a, b\}}(f)$, and they come about from the data at the limits of the angular range, a and b . Remarkably, if f has a singularity at one point on the circle $C(\phi, r)$ (for $\phi = a$ or $\phi = b$) conormal to the circle, then that singularity can be spread over the entire circle in the reconstruction.

Figure 2 illustrates this perfectly (as do the reconstructions in Section 5). The data are taken for $\phi \in [0, \pi]$. Every singularity in D is visible since, for every $x \in D$ and $\xi \in \mathbb{R}^2 \setminus \mathbf{0}$, there is a $\phi \in [0, \pi]$ with $\xi = \alpha \mathbf{n}(\phi, x)$ for some $\alpha \neq 0$; that is, for every covector $(x, \xi \mathbf{d}\mathbf{x}) \in T^*(D) \setminus \mathbf{0}$, there is a $\phi \in [0, \pi]$ such that $(x, \xi \mathbf{d}\mathbf{x})$ is conormal to the circle $C(\phi, \|x - \theta(\phi)\|)$.

The added singularities are as predicted by the theorem. They appear on circles $C(\phi, r)$ when $\phi = 0, \pi$, the endpoints of the interval of detectors and when some singularity of f is conormal to the circle. For the simple phantom in Figure 2 there are four circles of added artifacts, and they are tangent to the boundary of the object at points on the horizontal axis.

Next, we will show that the same artifact reduction procedure suggested in [11] is valid for this case, too. Let a' and b' be chosen so $a < a' < b' < b$ and choose a smooth cutoff function $\varphi : [0, 2\pi] \rightarrow \mathbb{R}$ supported in (a, b) and equal to one on $[a', b']$. Define the operator $\mathcal{K}_\varphi : \mathcal{D}'(\Xi) \rightarrow \mathcal{D}'(\Xi)$ by

$$\mathcal{K}_\varphi g = \varphi g. \quad (25)$$

Then $\mathcal{K}_\varphi \mathcal{M}$ uses only data for $\phi \in [a, b]$ but it provides a smooth cutoff. This discussion leads to the following theorem.

Theorem 4.4 (Reduction of Artifacts for the circular mean transform). *Let \mathcal{K}_φ be defined by (25) and let P be a pseudodifferential operator on $\mathcal{E}'(\Xi)$. Finally, let*

$$\mathcal{L}_\varphi = \mathcal{M}^* P \mathcal{K}_\varphi \mathcal{M},$$

then \mathcal{L}_φ is a standard smooth pseudodifferential operator. So, if $f \in \mathcal{E}'(D)$, then

$$\text{WF}(\mathcal{L}_\varphi(f)) \subset \text{WF}(f) \cap \mathcal{V}_{[a, b]}. \quad (26)$$

Thus, only visible singularities of f are visible in $\mathcal{L}_\varphi(f)$, and there are no added singularities. The proofs of these theorems are in the appendix.

4.2 Sonar (spherical mean transform with centers on a plane)

9

In this section, we analyze a limited data problem for sonar. We assume the sound speed is constant and there are not multiple reflections. Then, using the ansatz of Cohen and Bleistein [5] the data can be reduced to integrals over spheres centered on the ocean surface of the perturbation, $f(x)$, from the constant sound speed. We assume the ocean surface is planar and consider sonar data from transceivers on a compact subset, K , of that plane.

The functions we consider will be compactly supported in the open upper half plane

$$X := \{(x_1, x_2, x_3) \in \mathbb{R}^3 : x_3 > 0\}.$$

Let $\Xi_S := \mathbb{R}^2 \times (0, \infty)$, and denote the sphere centered at $(y, 0)$ and of radius r by

$$S(y, r) = \{x \in \mathbb{R}^3 : \|x - (y, 0)\| = r\}.$$

The spherical mean transform of $f \in \mathcal{D}(X)$ is denoted

$$\mathcal{M}_S f(y, r) = \frac{1}{4\pi r^2} \int_{x \in S(y, r)} f(x) dx, \quad (27)$$

where dx is the surface measure on the sphere $S(y, r)$. For $g \in \mathcal{E}'(\Xi_S)$, the dual transform is given by

$$\mathcal{M}_S^* g(x) = \int_{y \in \mathbb{R}^2} g(y, \|x - (y, 0)\|) \frac{1}{4\pi \|x - (y, 0)\|^2} dy,$$

where we note that the weight does not blow up since the integral is evaluated at $x \in X$.

Let K be a compact subset of \mathbb{R}^2 with nontrivial interior. We consider the limited data problem where data are given over spheres $S(y, r)$ with (y, r) in

$$A = K \times (0, \infty).$$

The resulting transform is

$$\mathcal{M}_{S,A} = \chi_A \mathcal{M}_S.$$

Since K is compact, for any $f \in \mathcal{E}'(X)$, $\mathcal{M}_{S,A}(f) \in \mathcal{E}'(\Xi_S)$.

For $x \in X$ and $y \in \mathbb{R}^2$, we let

$$\mathbf{n}(y, x) = \frac{x - (y, 0)}{\|x - (y, 0)\|} \quad (28)$$

denote the outward unit normal at x to the sphere $S(y, \|x - (y, 0)\|)$. Note that the third coordinate of $\mathbf{n}(y, x)$ is never equal to zero since $x_3 > 0$.

We define the set

$$\mathcal{V}_{S,K} := \{(x, \xi \mathbf{d}\mathbf{x}) \in T^*(X) : \exists y \in K, \exists \alpha \neq 0, \xi = \alpha \mathbf{n}(y, x)\}. \quad (29)$$

In our next theorem, we show $\mathcal{V}_{S,K}$ is the set of *possible visible singularities*, i.e., those that can be imaged by $\mathcal{M}_S^* P \mathcal{M}_{S,A}$ (singularities above points $y \in \text{bd}(K)$ might be cancelled).

If $x = (x_1, x_2, x_3) \in \mathbb{R}^3$ then we define $x' = (x_1, x_2)$.

Singularities are spread in more subtle ways in sonar than in TAT and so we need to introduce more notation to properly describe these added artifacts. Let S_+^2 denote the open top hemisphere of S^2 . Let $(y, r) \in \Xi_S$ and let $\eta \in \mathbb{R}^2 \setminus \mathbf{0}$ and $\mathbf{n} \in S_+^2$. Let $C(y, r, \eta, \mathbf{n})$ be the circle on $S(y, r)$

$$C(y, r, \eta, \mathbf{n}) = \{x \in S(y, r) : \exists a \in \mathbb{R}, x' - y = a\eta + r\mathbf{n}'\}. \quad (30)$$

This circle is the intersection of $S(y, r)$ with the vertical plane that is parallel to η and goes through $(y + r\mathbf{n}', 0)$.

Let $K \subset \mathbb{R}^2$ be a compact set bounded by a piecewise C^∞ , simple, closed curve, $B = \text{bd}(K)$. Then¹⁰ the singular support of χ_K is B . As noted in Example 2.1, at points $y \in B$ at which B is a smooth curve, $(y, \eta \mathbf{d}y) \in \text{WF}(\chi_K)$ if and only if η is normal to B at y . On the other hand, if B has a corner at y then all covectors above y are in $\text{WF}(\chi_K)$. By [31], $\text{WF}(\chi_K)$ is a set of covectors above $\text{bd}(K)$, and at any point $y \in \text{bd}(K)$ at which $\text{bd}(K)$ is smooth, they are the conormal covectors to $\text{bd}(K)$ at y (see the discussion in Example 2.1).

The following definition allows us to apply our next theorem to more general sets K than those with piecewise smooth boundaries.

Definition 4.5 (Generalized Normal Bundle). Let K be a compact subset of \mathbb{R}^2 . Define the *generalized normal bundle of K* to be the set, $N(K)$, of vectors in $\mathbb{R}^2 \times (\mathbb{R}^2 \setminus \mathbf{0})$ corresponding to covectors in the wavefront set of χ_K :

$$N(K) = \{(y, \eta) \in \mathbb{R}^2 \times (\mathbb{R}^2 \setminus \mathbf{0}) : (y, \eta \mathbf{d}y) \in \text{WF}(\chi_K)\}.$$

Using this notation and with $A = K \times (0, \infty)$, the wavefront set of χ_A as a function on Ξ_S is

$$\text{WF}(\chi_A) = \{(y, r), \eta \mathbf{d}y) : (y, \eta) \in N(K), r > 0\}.$$

If K is bounded by a smooth closed curve then our definition of $N(K)$ corresponds with the standard definition of the normal bundle of $\text{bd}(K)$. However, if K itself is a curve, then $\chi_K = 0$ as a distribution. This means that, by our definition $N(K) = \emptyset$, and this definition does not exactly correspond to the standard normal bundle of $\text{bd}(K) = K$.

Now, we introduce the set of added singularities. Let $f \in \mathcal{E}'(X)$ and let K a compact subset of \mathbb{R}^2 . Define the set

$$\begin{aligned} \mathcal{A}_{S,K}(f) := & \bigcup \left\{ \{(x, \alpha \mathbf{n}(y, x) \mathbf{d}x) : x \in C(y, r, \eta, \mathbf{n}(y, \tilde{x}))\} \right. \\ & \left. : (y, \eta) \in N(K), r > 0, \alpha \neq 0, \tilde{x} \in S(y, r) \text{ and } (\tilde{x}, \alpha \mathbf{n}(y, \tilde{x}) \mathbf{d}x) \in \text{WF}(f)\} \right\}. \end{aligned} \quad (31)$$

We will say more about this set after the theorem.

Theorem 4.6 (Visible and Added Singularities for the Spherical transform). *Let $f \in \mathcal{E}'(X)$ and let P be a properly supported pseudodifferential operator on $\mathcal{D}'(\Xi_S)$. Let K be a compact subset of \mathbb{R}^2 with nontrivial interior and let $A = K \times (0, \infty)$. Then,*

$$\text{WF}(\mathcal{M}_S^* P \mathcal{M}_{S,A} f) \subset (\text{WF}(f) \cap \mathcal{V}_{S,K}) \cup \mathcal{A}_{S,K}(f). \quad (32)$$

If P is elliptic on $\text{range}(\mathcal{M}_S)$, then,

$$\text{WF}(f) \cap \mathcal{V}_{S, \text{int}(K)} \subset \text{WF}(\mathcal{M}_S^* P \mathcal{M}_{S,A} f). \quad (33)$$

Remark 4.7. In practice, K will be a compact set bounded by a simple piecewise smooth curve, and we now consider $\mathcal{A}_{S,K}(f)$ in this case. By the definition of $\mathcal{A}_{S,K}(f)$ and Theorem 4.6, singularities are added on spheres $S(y, r)$. For added singularities to appear on $S(y, r)$ the following must be satisfied:

- $y \in \text{bd}(K)$
- There is an $\tilde{x} \in S(y, r)$ and $\alpha \neq 0$ with $(\tilde{x}, \alpha \mathbf{n}(y, \tilde{x}) \mathbf{d}x) \in \text{WF}(f)$.

Once this is true, the singularities spread differently depending on the geometry of $\text{bd}(K)$. Let $y \in \text{bd}(K)$, $r > 0$, and $\alpha \neq 0$. Assume $\tilde{x} \in S(y, r)$ with $(\tilde{x}, \alpha \mathbf{n}(y, \tilde{x}) \mathbf{d}x) \in \text{WF}(f)$.

First, assume $\text{bd}(K)$ is a smooth curve at y . Let η be a normal to $\text{bd}(K)$ at y , then all normals to $\text{bd}(K)$ at y are parallel to η . Thus, the added singularities caused by the singularity of f at $(\tilde{x}, \alpha \mathbf{n}(y, \tilde{x}) \mathbf{d}x)$ will be on the semicircle $C(y, r, \eta, \alpha \mathbf{n}(y, \tilde{x})) \cap X$ but nowhere else on $S(y, r)$.

Now assume that $\text{bd}(K)$ has a corner at y . Then, for all $\eta \neq 0, (y, \eta) \in N(K)$. Each such η generates a semicircle of possible added singularities that is in a plane parallel to η and through the fixed point

$(y + r\mathbf{n}'(y, \tilde{x}), 0)$. As η changes, this semicircle sweeps out the entire hemisphere $S(y, r) \cap X$. Thus, in this case, added singularities are on this entire hemisphere.

This discussion justifies using measurement sets K with smooth boundaries so added singularities do not spread along entire hemispheres.

These theorems do not address what happens to “boundary singularities” of f , namely those for covectors $(x, \xi \mathbf{d}\mathbf{x}) \in \mathcal{V}_{\text{bd}(K)}$. In general, these singularities can be invisible or visible.

The reconstruction from simulated sonar data in Figure 3, which was taken from [34], illustrate our theorem perfectly; there are added singularities in exactly the places predicted by the theorem. In fact, all of the reconstructions in [34] have the added artifacts in the locations predicted by the theorem.

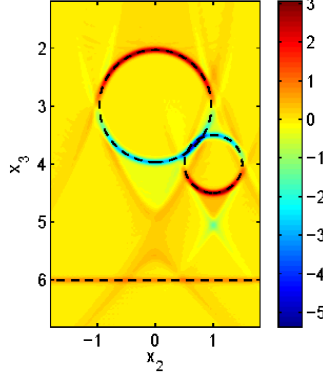


Figure 3: Reconstruction from spherical mean data of the characteristic functions of two balls and a horizontal ocean floor. The center set $K = [-12, 12]^2$ and the reconstruction is in the plane $x_1 = 0.25$. The spheres are centered at $(0, 0, 3)$ and $(0, 1, 4)$. The added artifacts in this picture are along circles parallel the $x_2 x_3$ plane (since they are caused by normals perpendicular to the x_1 axis for spheres centered on lines parallel the x_1 axis). Note that the predicted artifact caused by the ocean floor would be outside the reconstruction region since it would be caused by spheres centered at $(0.25, \pm 12, 0)$ and of radius 6. Reprinted from [34] by permission of IOP Publishing.

The same artifact reduction procedure suggested in [11] is valid for this case, too. Let K' be an open set whose closure is contained in $\text{int}(K)$ and let $\varphi : \mathbb{R}^2 \rightarrow \mathbb{R}$ be a smooth cutoff function that is supported in $\text{int}(K)$ and equal to one on K' . In this case, the operator $\mathcal{K}_\varphi : \mathcal{D}'(\Xi_S) \rightarrow \mathcal{D}'(\Xi_S)$ is

$$\mathcal{K}_\varphi g = \varphi g.$$

Then $\mathcal{K}_\varphi \mathcal{M}_S$ uses only data for $y \in K$ but it provides a smooth cutoff. This discussion leads to the following theorem.

Theorem 4.8 (Reduction of Artifacts for the sonar transform). *Let K be a compact subset of \mathbb{R}^2 with nontrivial interior. Let P be a properly supported pseudodifferential operator on $\mathcal{E}'(\Xi_S)$. Let K' be an open set whose closure is contained in $\text{int}(K)$ and let $\varphi : \mathbb{R}^2 \rightarrow \mathbb{R}$ be a smooth function supported in $\text{int}(K)$ and equal to one on K' . Let*

$$\mathcal{L}_\varphi = \mathcal{M}_S^* P \mathcal{K}_\varphi \mathcal{M}_S,$$

then \mathcal{L}_φ is a standard C^∞ pseudodifferential operator and so

$$\text{WF}(\mathcal{L}_\varphi(f)) \subset \text{WF}(f) \cap \mathcal{V}_{S,K}$$

for $f \in \mathcal{E}'(X)$. If P is elliptic on $\text{range}(\mathcal{M}_S)$, then \mathcal{L}_φ is elliptic on $\mathcal{V}_{S,K'}$, so, if $f \in \mathcal{E}(D)$, then

$$\text{WF}(f) \cap \mathcal{V}_{S,K'} \subset \text{WF}(\mathcal{L}_\varphi(f)) \subset \text{WF}(f) \cap \mathcal{V}_{S,K}. \quad (34)$$

Thus, only visible singularities of f are visible in $\mathcal{L}_\varphi(f)$, and there are no added singularities. In contrast¹² to the circular mean case, when P is elliptic, all of the singularities of f in $\mathcal{V}_{S,K'}$ are visible in $\mathcal{L}_\varphi(f)$. This difference will be explained in Remark A.1.

5 Numerical Examples

In this section we illustrate the capability of our artifact reduction strategy for limited view reconstruction from circular mean data. In particular, we show that the proposed artifact reduction strategy performs very well on synthetic data as well as on real photoacoustic data. In our experiments we consider the circular mean transform, \mathcal{M} , with detectors on a circle or circular arc surrounding the object. This is the standard model in sectional imaging in photo- and thermoacoustic tomography [6, 35], and it is the model we analyzed in Section 4.1. The Sonar case, as presented in Section 4.2, can be implemented similarly and we expect similar results.

For the numerical experiments, we implemented the following reconstruction operators in Matlab,

$$\mathcal{L}^1 = \mathcal{M}^* \left(\frac{d}{dr} \right) \mathcal{M}, \quad \mathcal{L}^2 = \mathcal{M}^* \left(-\frac{d^2}{dr^2} \right) \mathcal{M}. \quad (35)$$

We also implemented their artifact reduced versions

$$\mathcal{L}_\varphi^1 = \mathcal{M}^* \left(\frac{d}{dr} \right) \mathcal{K}_\varphi \mathcal{M}, \quad \mathcal{L}_\varphi^2 = \mathcal{M}^* \left(-\frac{d^2}{dr^2} \right) \mathcal{K}_\varphi \mathcal{M}, \quad (36)$$

where \mathcal{K}_φ is the multiplication operator defined in (25). \mathcal{K}_φ multiplies the limited view data $g = \mathcal{M}_{[a,b]}f$ with a smooth truncation function φ that satisfies the assumptions of Theorem 4.4. In our implementation of \mathcal{K}_φ we use a similar cutoff function as in [11]. Namely, we choose $\varepsilon \in (0, (b-a)/2)$ let $\varphi = \varphi_\varepsilon : [0, 2\pi] \rightarrow \mathbb{R}$ be supported in $[a, b] \subset [0, 2\pi]$ so that $\varphi(\phi) = 1$ for $\phi \in [a + \varepsilon, b - \varepsilon] \subset [a, b]$. In the transition regions, $[a, a + \varepsilon]$ and $[b - \varepsilon, b]$, we used the function ν_ε defined by $\nu_\varepsilon(x) = \exp(\frac{x^2}{x^2 - \varepsilon^2})$ for $|x| < \varepsilon$ and $\nu_\varepsilon(x) = 0$ for $|x| \geq \varepsilon$, to generate a smooth transition from 0 to 1 and from 1 to 0, respectively. That is, for $\phi \in [a, a + \varepsilon]$ we set $\varphi_\varepsilon(\phi) = \nu_\varepsilon(a + \varepsilon - \phi)$, and for $\phi \in [b - \varepsilon, b]$ we set $\varphi_\varepsilon(\phi) = \nu_\varepsilon(\phi - b + \varepsilon)$. The function φ_ε defines a smooth function apart from $\phi = a + \varepsilon$ and $\phi = b - \varepsilon$. Even though this function is not globally smooth, we may use it for artifact reduction because, in practice, it is evaluated at a finite number of points and there is a smooth function that has these values at these points. Moreover, this function has shown to provide good artifact reduction results in limited angle x-ray tomography, cf. [11].

In our experiments, we performed two sets of reconstructions. In our first experiment, we computed reconstructions from synthetic data. Here, we generated limited view spherical mean data $g = \mathcal{M}_{[a,b]}f$ in Matlab from a characteristic function of a circle centered around the origin and from the Forbild head phantom [22]. The corresponding Lambda type reconstructions $\mathcal{L}^2 g$ and $\mathcal{L}_\varphi^2 g$ are shown in Figures 1 and 4. The standard reconstructions $\mathcal{L}^2 g$ without artifact reduction (left images) clearly show the circular artifacts as characterized in Section 4.1, see also Figure 2. In particular, in the $\mathcal{L}^2 g$ reconstruction of Figure 4, we observe that many artifacts overlap and significantly degrade the reconstruction quality (even generating new image features). This is due to the presence of many singularities in the original image. Thus, similar behavior can be expected for any limited view reconstruction of an image with many singularities. By using artifact reduced reconstruction operators $\mathcal{L}_\varphi^2 g$, in Figures 1 and 4, we can clearly observe an improvement of image quality. The artifacts are clearly reduced while most of the visible singularities are preserved (even this could not be proven in Section 4.1, see Remark A.1). However, we also observe that some of the visible singularities with directions at the boundary of the limited view are smoothed.

In our second experiment, we computed reconstructions from real photoacoustic measurements. More precisely, we computed the backprojection of the experimental pressure data that were generated through a focused illumination of the object in the plane $z = 0$, and measured by acoustic detectors that were distributed on a circular arc surrounding the object. The data is by courtesy of the group of Prof. Daniel Razansky (Institute for Biological and Medical Imaging, Helmholtz Zentrum München). For more details on

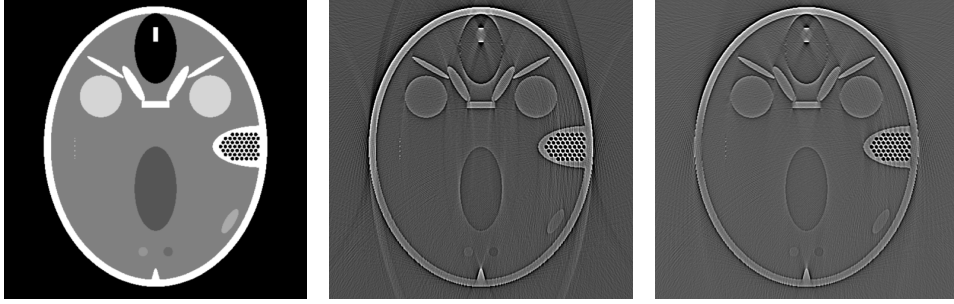


Figure 4: Lambda type reconstruction (512×512) of the FORBILD head phantom [22] for the limited angular range $[0^\circ, 180^\circ]$ (750 projections, 725 radii). The left-hand picture is the original phantom, the middle picture is the reconstruction without artifact reduction and the right-hand picture is an artifact reduced reconstruction with $\varepsilon = 18^\circ$.

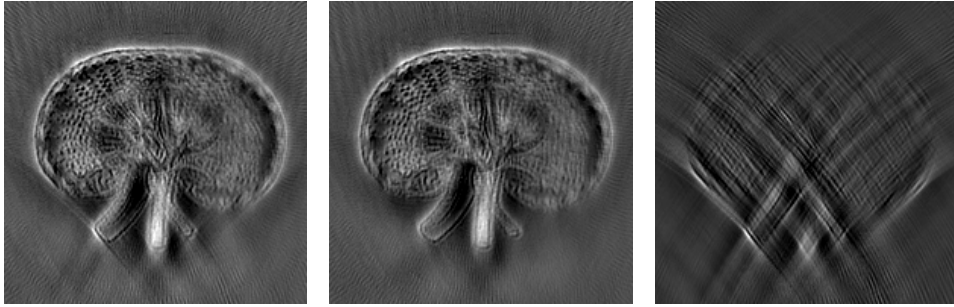


Figure 5: Real data reconstruction (200×200) of a paper phantom with ink as an optical absorber for the limited angular range $[-45^\circ, 225^\circ]$ (256 projections, 2030 radii). *Left:* $\mathcal{L}^1 g$ (no artifact reduction); *Middle:* $\mathcal{L}^1_\varphi g$ with $\varepsilon = 45^\circ$ (reconstruction with artifact reduction); *Right:* $|\mathcal{L}^1 g - \mathcal{L}^1_\varphi g|$ (difference image). In above reconstructions one can clearly observe the effect of artifact reduction. The difference image shows that the geometry of artifacts corresponds to the theoretical characterization of Section 4.1.

the measurement setup we refer to [35]. Although real PAT data is three dimensional in nature, the pressure data p (measured in the plane $z = 0$) of the described sectional imaging setup is related to the circular mean operator by $p(\xi, t) = \frac{1}{2} \partial_t \mathcal{M}f(\xi, t)$, where $\mathcal{M}f(\xi, t)$ denote the circular means of the imaged section, for more details see [6]. Thus, our reconstructions correspond to the application of the operators \mathcal{L}^1 and \mathcal{L}^1_φ to the limited view circular mean data $g = \mathcal{M}_{[a,b]}f$.

The images of Figure 5 show reconstructions of a paper phantom (which has ink as an optical absorber) and images in Figure 6 show reconstructions of a mouse tumor. In Figure 5, one can clearly observe the effect of artifact reduction induced by smooth truncation of the limited view data at the ends of the angular range. As previously, the visible singularities are well preserved while the circular artifacts are removed as can be seen from the difference image in Figure 5. We would like to point out that even though the ground truth is not available the theoretical analysis of Section 4 together with previous examples enable us to differentiate between reliable image features and added artifacts (which are located on circular arcs). This is very important since there are practical situations where it is not that easy to distinguish between reliable image features and artifacts. For example, Figure 6 shows another limited view reconstruction from experimental photoacoustic data where the artifacts are not as distinctive as in Figure 5. The reconstruction with artifact reduction is presented in the middle image of Figure 6. Here, one can observe that a superior image quality is achieved through the application of artifact reduction: the reconstructions appear to be more clear, having a more homogeneous background. As seen from the difference image in Figure 6 the circular artifacts are removed effectively.

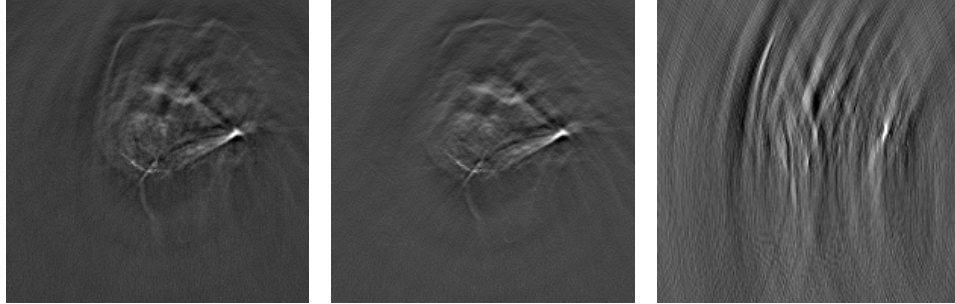


Figure 6: Real data reconstruction (200×200 , 2193 radii) of a mouse tumor for the limited angular range $[0^\circ, 180^\circ]$ (200 projections). *Left*: $\mathcal{L}^1 g$ (no artifact reduction); *Middle*: $\mathcal{L}^1_{\varphi} g$ with $\varepsilon = 45^\circ$ (reconstruction with artifact reduction); *Right*: $|\mathcal{L}^1 g - \mathcal{L}^1_{\varphi} g|$ (difference image). Though in the left image the added artifacts are not clearly distinguishable from reliable image features one clearly observes an increase of image quality by using the reconstruction operator with artifact reduction. The difference image shows that artifacts are effectively removed and that the geometry of the artifacts is in accordance with the theoretical characterizations, see also Figure 2.

Finally, we note that the visibility of artifacts in numerical reconstructions highly depends on the choice of the ε -parameter in the cutoff function (φ_ε above). For a detailed discussion we refer to [11]. Here, we note only that there is a trade-off between mitigation of artifacts and smoothing of visible singularities: large ε -parameters lead to good mitigation of artifacts in the reconstruction while at the same time (depending on the limited view) a large ε -parameter can smooth the visible singularities, as in Figures 1 and 4. In contrast, small ε -parameters preserve most of the visible singularities while circular artifacts might still be clearly visible. In all of the above experiments, we have chosen the “optimal” ε -parameter by visually inspecting a series of reconstructions with different parameters.

To sum up, our theoretical analysis of Section 4 helps to distinguish between reliable image features and artifacts in limited view reconstructions (thus improving proper interpretation of limited view reconstructions). In particular, it provides an effective and easy-to-implement strategy for artifact reduction. Our experiments show that this strategy significantly improves the reconstruction quality not only in reconstructions from synthetic phantom data but also from real experimental data.

6 Concluding Remarks

In this paper we presented a paradigm to precisely characterize potential added singularities in limited data tomography problems. The paradigm in Section 3 is general and can be applied to a range of other limited data problems besides limited angle tomography, and the ones we studied in this article: PAT/TAT and Sonar. We proved that these added singularities come from data at the boundary of the data set. For PAT/TAT with data on $[a, b] \times (0, 2)$, if the object, f , has a singularity on a circle $C(a, r)$ or $C(b, r)$ that is conormal to the circle, then the singularity can be spread over the entire circle (see Remark 4.3). In Sonar with limited data on $K \times (0, \infty)$, the added artifacts appear on part or all of the spheres $S(y, r)$ for $y \in \text{bd}(K)$. If f has a singularity conormal to such a sphere, then singularities can be spread along a circle on that sphere if $\text{bd}(K)$ is smooth at y and along the entire sphere if $\text{bd}(K)$ is not smooth at y (see Remark 4.7).

For the case of sonar we showed that detector locations (the set A) with smooth boundaries will produce fewer added artifacts than sets with corners.

Moreover, we showed that, with a smooth cutoff at the boundary, the added artifacts are eliminated. Reconstructions from real and simulated data were presented that illustrate our paradigm and the artifact reduction procedure.

The first author thanks Tufts University for its hospitality during the during the spring semester 2014 when most of the presented work was done. Moreover, he acknowledges support by the Helmholtz Association within the young investigator group VH-NG-526. The second author was supported by NSF grant DMS1311558 as well as the generosity of the Technische Universität München and the Helmholtz Zentrum, München. The second author thanks Jan Boman for many enlightening discussions about microlocal analysis over the years as well a helpful observation about wavefront of real-valued functions that is used in the proof of Theorem 4.6. We thank Anuj Abhishek for his helpful comments on ideas in this article. The authors thank Clifford Nolan for insightful discussions about this research and seismic imaging. They thank Frank Filbir and Stefan Kunis for encouraging and supporting this collaboration. The authors thank Daniel Queiros and the group of Prof. Daniel Razansky (both at the Institute for Biological and Medical Imaging, Helmholtz Zentrum München) for providing us experimental photoacoustic data.

Finally, the authors are indebted to the referees for their thoughtful comments that improved the article.

A Proofs of Theorems 4.2, 4.4, 4.6, and 4.8

Proof of Theorem 4.2. We prove the theorem by going through the paradigm discussed in section 3 using Lemma 3.2.

The canonical relation of \mathcal{M} is given in equations (4.2)-(4.4) in the proof of Lemma 4.3 on p. 396 of [1].

$$C_{\mathcal{M}} = \left\{ ((\phi, r), \alpha [\theta^\perp(\phi) \cdot \mathbf{n}(\phi, x) \mathbf{d}\phi + \mathbf{d}\mathbf{r}]; x, \alpha \mathbf{n}(\phi, x) \mathbf{d}\mathbf{x}) : \right. \\ \left. \alpha \neq 0, (\phi, r) \in \Xi, x \in C(\phi, r) \cap D \right\} \quad (37)$$

where $\theta^\perp(\phi) = \theta(\phi + \pi/2)$ is perpendicular to $\theta(\phi)$.

Recall that $A = [a, b] \times (0, \infty)$ in this proof. The non-cancellation condition (11) in Theorem 3.1 holds since $\text{WF}(\chi_A)$ has $\mathbf{d}\mathbf{r}$ component of zero, and any covector in $C_{\mathcal{M}} \circ (T^*(D) \setminus \mathbf{0})$ has nonzero $\mathbf{d}\mathbf{r}$ component. So, this theorem can be used to show that the product $\chi_{[a,b]} \mathcal{M}$ is well-defined for distributions $f \in \mathcal{E}'(D)$ and

$$\text{WF}(\chi_{[a,b]} \mathcal{M} f) \subset \mathcal{Q}(A, C_{\mathcal{M}} \circ \text{WF}(f))$$

(see (14)). We calculate $\mathcal{Q}(A, \text{WF}(C_{\mathcal{M}} \circ \text{WF}(f)))$ in steps.

Using (37) we see

$$C_{\mathcal{M}} \circ \text{WF}(f) = \left\{ ((\phi, r), \alpha [\theta^\perp(\phi) \cdot \mathbf{n}(\phi, x) \mathbf{d}\phi + \mathbf{d}\mathbf{r}]) : \right. \\ \left. (\phi, r) \in \Xi, \alpha \neq 0, \exists x \in C(\phi, r), (x, \alpha \mathbf{n}(\phi, x) \mathbf{d}\mathbf{x}) \in \text{WF}(f) \right\}. \quad (38)$$

According to the definition of \mathcal{Q} , (13),

$$\mathcal{Q}(A, C_{\mathcal{M}} \circ \text{WF}(f)) = \{ ((\phi, r), \xi + \eta) : \phi \in [a, b], [((\phi, r), \xi) \in C_{\mathcal{M}} \circ \text{WF}(f) \text{ or } \xi = 0] \\ \text{and } [((\phi, r), \eta) \in \text{WF}(\chi_A) \text{ or } \eta = 0] \} \quad (39)$$

One can break the right-hand side of (39) into the union of three sets:

$$\mathcal{Q}(A, C_{\mathcal{M}} \circ \text{WF}(f)) = [(C_{\mathcal{M}} \circ \text{WF}(f)) \cap \{(\phi, r, \eta) \in T^*(\Xi) : \phi \in [a, b]\}] \quad (40)$$

$$\cup \text{WF}(\chi_A) \cup W_{\{a,b\}}(f) \quad (41)$$

where the set

$$W_{\{a,b\}}(f) = \left\{ ((\phi, r), [\mu + \alpha \theta^\perp(\phi) \cdot \mathbf{n}(\phi, \tilde{x}) \mathbf{d}\phi + \alpha \mathbf{d}\mathbf{r}]) : \right. \\ \left. \alpha, \mu \neq 0, \phi \in \{a, b\}, r \in (0, \infty) \exists \tilde{x} \in C(\phi, r), (\tilde{x}, \alpha \mathbf{n}(\phi, \tilde{x}) \mathbf{d}\mathbf{x}) \in \text{WF}(f) \right\}.$$

is generated by terms $\xi \neq 0$ and $\eta \neq 0$ in (39). Furthermore, $W_{\{a,b\}}(f)$ can be written

16

$$W_{\{a,b\}}(f) = \left\{ ((\phi, r), \nu \mathbf{d}\phi + \alpha \mathbf{d}\mathbf{r}) : \phi \in \{a, b\}, \nu \in \mathbb{R}, \alpha \neq 0, \right. \\ \left. \exists \tilde{x} \in C(\phi, r), (\tilde{x}, \alpha \mathbf{n}(\phi, \tilde{x}) \mathbf{d}\mathbf{x}) \in \text{WF}(f) \right\}. \quad (42)$$

because $\nu = \mu + \alpha \theta^\perp(\phi) \cdot \mathbf{n}(\phi, \tilde{x})$ is arbitrary since, for $\phi \in \{a, b\}$, every nonzero covector $((\phi, r), \mu \mathbf{d}\phi) \in \text{WF}(\chi_A)$ (we allow $\mu = 0$ in this expression to make the proof easier to describe). At this point, we have finished steps (a) to (d) of the paradigm of Section 3.

In the next step we compute $C_{\mathcal{M}}^t \circ \mathcal{Q}(A, C_{\mathcal{M}} \circ \text{WF}(f))$ by first finding explicit expressions for the compositions with $C_{\mathcal{M}}$ and $C_{\mathcal{M}}^t$.

For $(x, \xi) \in D \times (\mathbb{R}^2 \setminus \mathbf{0})$ define ϕ_1 as the unique angle in $[0, 2\pi]$ such that $\theta(\phi_1)$ is the intersection of S^1 with the ray $\{x + t\xi : t < 0\}$ and define ϕ_2 as the unique angle in $[0, 2\pi]$ such that $\theta(\phi_2)$ is the intersection of S^1 with the ray $\{x + t\xi : t > 0\}$. Note that ϕ_1 and ϕ_2 are smooth functions of $(x, \xi \mathbf{d}\mathbf{x})$. Define for $j = 1, 2$

$$\alpha_1(\xi) = \|\xi\| \quad \alpha_2(\xi) = -\|\xi\|, \quad r_j(x, \xi) = \|x - \theta(\phi_j(x, \xi))\|, \\ c_j(x, \xi \mathbf{d}\mathbf{x}) = ((\phi_j(x, \xi), r_j(x, \xi)), \alpha_j(x, \xi) [\mathbf{n}(\phi_j(x, \xi), x) \cdot \theta^\perp(\phi_j(x, \xi)) \mathbf{d}\phi + \mathbf{d}\mathbf{r}])$$

then $C_{\mathcal{M}} \circ \{(x, \xi \mathbf{d}\mathbf{x})\} = \{c_j(x, \xi \mathbf{d}\mathbf{x}) : j = 1, 2\}$.

Let $\nu \in \mathbb{R}, \alpha \neq 0$ and assume $\nu/\alpha \in [-1, 1]$. Define

$$x((\phi, r), \nu, \alpha) = \theta(\phi) + r \left((\nu/\alpha) \theta^\perp(\phi) - \sqrt{1 - (\nu/\alpha)^2} \theta(\phi) \right), \\ \xi((\phi, r), \nu, \alpha) = \alpha \mathbf{n}(\phi, x((\phi, r), \nu, \alpha)). \quad (43)$$

Note that $x((\phi, r), \nu, \alpha) \in C(\phi, r)$ and if ν/α and r are sufficiently close to zero, this point is in D . Define

$$T_{\mathcal{M}} = \{((\phi, r), \nu \mathbf{d}\phi + \alpha \mathbf{d}\mathbf{r}) : (\phi, r) \in \Xi, \alpha \neq 0, \nu/\alpha \in [-1, 1], x((\phi, r), \nu, \alpha) \in D\}.$$

Then, $c_j : T^*(D) \setminus \mathbf{0} \rightarrow T_{\mathcal{M}}$ and $c_1(T^*(D) \setminus \mathbf{0}) \cup c_2(T^*(D) \setminus \mathbf{0}) = T_{\mathcal{M}}$. These statements are proven using geometry and the observations that $x_\phi = x((\phi, r), \nu, \alpha)$ satisfies $(\mathbf{n}(\phi, x_\phi) \cdot \theta^\perp(\phi) = \nu/\alpha$ and $x_\phi \in C(\phi, r)$.

For $\nu/\alpha \in [-1, 1]$ and $(\phi, r) \in \Xi$, whenever $x((\phi, r), \nu, \alpha) \in D$, define

$$c_{\text{inv}}((\phi, r), \nu, \alpha) = (x((\phi, r), \nu, \alpha), \xi((\phi, r), \nu, \alpha) \mathbf{d}\mathbf{x}), \\ \text{then } \{c_{\text{inv}}((\phi, r), \nu, \alpha)\} = C_{\mathcal{M}}^t \circ \{((\phi, r), \nu \mathbf{d}\phi + \alpha \mathbf{d}\mathbf{r})\}. \quad (44)$$

These calculations allow one to show for $j = 1, 2$ that $c_{\text{inv}} \circ c_j$ is the identity map on $T^*(D) \setminus \mathbf{0}$. So, if $(x, \xi \mathbf{d}\mathbf{x}) \in T^*(D) \setminus \mathbf{0}$ then

$$C_{\mathcal{M}}^t \circ C_{\mathcal{M}} \{(x, \xi \mathbf{d}\mathbf{x})\} = \{(x, \xi \mathbf{d}\mathbf{x})\}. \quad (45)$$

Now that these basic observations have been made, we can calculate the wavefront set of $\mathcal{M}^* P\mathcal{M}_{[a,b]}(f)$. Using the composition rules (7), Theorem 2.4, and (40) yields the following union of sets:

$$C_{\mathcal{M}}^t \circ \mathcal{Q}(A, C_{\mathcal{M}} \circ \text{WF}(f)) = C_{\mathcal{M}}^t \circ [(C_{\mathcal{M}} \circ \text{WF}(f)) \cap \{(\phi, r, \eta) \in T^*(\Xi) : \phi \in [a, b]\}] \quad (46)$$

$$\cup C_{\mathcal{M}}^t \circ \text{WF}(\chi_A) \quad (47)$$

$$\cup C_{\mathcal{M}}^t \circ W_{\{a,b\}}(f) \quad (48)$$

We examine the three terms of (46)-(48) separately and we first show that the set in equation (46) is equal to $\mathcal{V}_{[a,b]} \cap \text{WF}(f)$. Let $(x_0, \xi_0 \mathbf{d}\mathbf{x})$ be in the set in (46). Then $(x_0, \xi_0 \mathbf{d}\mathbf{x}) \in C_{\mathcal{M}}^t \circ (C_{\mathcal{M}} \circ \text{WF}(f)) = \text{WF}(f)$ by (45). Because $(x_0, \xi_0 \mathbf{d}\mathbf{x})$ is also in the set

$$C_{\mathcal{M}}^t \circ \{(\phi, r, \eta) \in T^*(\Xi) : \phi \in [a, b]\},$$

either $\phi_1(x_0, \xi_0)$ or $\phi_2(x_0, \xi_0)$ (or both) must be in $[a, b]$. Therefore, $\xi_0 = \alpha \mathbf{n}(\phi, x_0)$ for some $\phi \in [a, b]$ and some $\alpha \neq 0$. This means that $(x_0, \xi_0 \mathbf{dx}) \in \mathcal{V}_{[a,b]}$ and the set in (46) is contained in $\mathcal{V}_{[a,b]} \cap \text{WF}(f)$. The reverse containment is proven in a similar way.

Next, we consider the set in (47). As the \mathbf{dr} component of any covector in $\text{WF}(\chi_A)$ is zero and covectors in $C_{\mathcal{M}}^t$ all have nonzero \mathbf{dr} component, $C_{\mathcal{M}}^t \circ \text{WF}(\chi_A) = \emptyset$.

Finally, we consider the set $C_{\mathcal{M}}^t \circ W_{\{a,b\}}(f)$. Let $((\phi, r), \nu \mathbf{d}\phi + \alpha \mathbf{dr}) \in W_{\{a,b\}}(f)$. Then $\phi \in \{a, b\}$, $\nu \in \mathbb{R}$ is arbitrary, $\alpha \neq 0$, and for some $\tilde{x} \in C(\phi, r)$, $(\tilde{x}, \alpha \mathbf{n}(\phi, \tilde{x}) \mathbf{dx}) \in \text{WF}(f)$. For $C_{\mathcal{M}}^t \circ ((\phi, r), \nu \mathbf{d}\phi + \alpha \mathbf{dr})$ to be nonempty, ν/α can be any value in $[-1, 1]$ such that $x_\phi = x((\phi, r), \nu, \alpha) \in D$. Since r is fixed, x_ϕ is an arbitrary point on $C(\phi, r) \cap D$. This means that for every $x \in C(\phi, r) \cap D$, the covector $(x, \alpha \mathbf{n}(\phi, x) \mathbf{dx}) \in C_{\mathcal{M}}^t \circ W_{\{a,b\}}(f)$. Therefore, the set of possible added singularities from (48) is the set $\mathcal{A}_{\{a,b\}}(f)$ defined in (23).

Finally, we use Lemma 3.2 and the general wavefront containment (15) to conclude (24) in Theorem 4.2. This finishes the proof. \square

Proof of Theorem 4.4. Because \mathcal{K}_φ is a (trivial) pseudodifferential operator on $\mathcal{D}'(\Xi)$, $\mathcal{K}_\varphi \mathcal{M}$ is a standard C^∞ FIO with the same canonical relation as \mathcal{M} . Therefore, \mathcal{L}_φ is a standard pseudodifferential operator for distributions supported in D because

$$C_{\mathcal{M}}^t \circ C_{\mathcal{M}} = \Delta \quad (49)$$

is the diagonal in $T^*(D)$ (see [38]) by equation (45). So, $\text{WF}(\mathcal{L}_\varphi f) \subset \text{WF}(f)$ for any $f \in \mathcal{E}'(D)$.

To show the inclusion in (34), we note that if $(x_0, \xi_0 \mathbf{dx}) \notin \mathcal{V}_{[a,b]}$, then neither of the two angles $\phi_1 = \phi_1(x_0, \xi_0)$ and $\phi_2 = \phi_2(x_0, \xi_0)$ is in $[a, b]$. Therefore $\mathcal{K}_\varphi \mathcal{M}(f)$ is zero (and so smooth) near ϕ_j for $j = 1, 2$ and for any η above (ϕ_j, r) . That means that any covector above the point $(\phi_j, \|x_0 - \theta(\phi_j)\|)$ ($j = 1, 2$) is not in $\text{WF}(\mathcal{K}_\varphi \mathcal{M}(f))$. By (44), the only two covectors that could contribute to $C_{\mathcal{M}}^t \circ \text{WF}(\mathcal{K}_\varphi \mathcal{M}(f))$ at $(x_0, \xi_0 \mathbf{dx})$ are above these two points. Since $\text{WF}(\mathcal{L}_\varphi(f)) \subset C_{\mathcal{M}}^t \circ \text{WF}(\mathcal{K}_\varphi \mathcal{M}(f))$, $(x_0, \xi_0 \mathbf{dx}) \notin \text{WF}(\mathcal{L}_\varphi(f))$, this proves the theorem. \square

Proof of Theorem 4.6. We will recall some of the microlocal analysis of the sonar transform that was proven in [34]. The canonical relation of \mathcal{M}_S is [34, equation (3.5)]

$$C_S = \{ ((y, r), \alpha [\mathbf{n}'(y, x) \mathbf{dy} + \mathbf{dr}], x, \alpha \mathbf{n}(y, x) \mathbf{dx}) : (y, r) \in \Xi_S, x \in S(y, r) \cap X, \alpha \neq 0 \}. \quad (50)$$

Because $x_3 > 0$, $\xi = \alpha \mathbf{n}(y, x)$ always has $\xi_3 \neq 0$. Note that in equation (3.5) in [34] the \mathbf{dx} coordinate should be $+\alpha \mathbf{n}(y, x) \mathbf{dx}$ since C is the canonical relation for \mathcal{M}_S , not its Lagrangian manifold.

Let $(x, \xi \mathbf{dx}) \in T^*(X)$ with $\xi_3 \neq 0$. We define

$$c(x, \xi \mathbf{dx}) = (y(x, \xi), r(x, \xi), \alpha(x, \xi) [\omega'(\xi) \mathbf{dy} + \mathbf{dr}]) \quad (51)$$

where

$$\begin{aligned} y(x, \xi) &= \left(x - \frac{x_3}{\xi_3} \xi \right)' & r(x, \xi) &= \frac{x_3}{|\xi_3|} \|\xi\| \\ \alpha(\xi) &= \frac{\xi_3}{|\xi_3|} \|\xi\| & \omega(\xi) &= \frac{\xi_3}{|\xi_3| \|\xi\|} \xi \in S_+^2 \end{aligned} \quad (52)$$

and S_+^2 is the open upper hemisphere of S^2 .

Recall that $(x_1, x_2, x_3)' = (x_1, x_2)$. Then, by equations (3.7)-(3.10) in [34],

$$C_S \circ \{(x, \xi \mathbf{dx})\} = \{c(x, \xi \mathbf{dx})\}. \quad (53)$$

Note that c is a diffeomorphism from $\{(x, \xi) : x \in X, \xi_3 \neq 0\}$ onto

$$T_S = \{((y, r), \alpha[\eta \mathbf{dy} + \mathbf{dr}]) : (y, r) \in \Xi_S, \alpha \neq 0, \eta \in D\} \subset T^*(\Xi_S) \quad (54)$$

where D is the open unit disk in \mathbb{R}^2 .

Let $((y, r), \nu \mathbf{d}y + \alpha \mathbf{d}r) \in T_S$, Then, $\nu/\alpha \in D$ and so

$$\bar{n}(\nu, \alpha) = \left(\nu/\alpha, \sqrt{1 - \|\nu/\alpha\|^2} \right) \in S_+^2 \quad \text{and} \quad x(y, r, \nu, \alpha) = (y, 0) + r \bar{n}(\nu, \alpha)$$

satisfy

$$c^{-1}(((y, r), \nu \mathbf{d}y + \alpha \mathbf{d}r)) = (x(y, r, \nu, \alpha), \alpha \bar{n}(\nu, \alpha) \mathbf{d}x). \quad (55)$$

Because of relation (55) and the definition of C_S^t , if $((y, r), \nu \mathbf{d}y + \alpha \mathbf{d}r) \in T_S$ then

$$C_S^t \circ \{((y, r), \nu \mathbf{d}y + \alpha \mathbf{d}r)\} = \{c^{-1}((y, r), \nu \mathbf{d}y + \alpha \mathbf{d}r)\}.$$

Therefore,

$$C_S^t \circ C_S = \{(x, \xi \mathbf{d}x; x, \xi \mathbf{d}x) : x \in X, \xi_3 \neq 0\} \quad (56)$$

is a dense open subset of the diagonal $\Delta \subset T^*(X \times X)$. This finishes the general microlocal analysis of \mathcal{M}_S and \mathcal{M}_S^* .

Let $f \in \mathcal{E}'(X)$ and let K be a compact set in the plane with nontrivial interior and let $A = K \times (0, \infty)$.

Because every covector in T_S has nonzero $\mathbf{d}r$ component and every covector in $\text{WF}(\chi_A)$ has zero $\mathbf{d}r$ component, the non-cancellation condition (11) holds. So, by Theorem 3.1 the product $\chi_A \mathcal{M}_S f = \mathcal{M}_A(f)$ is a distribution. By Lemma 3.2, $\text{WF}(\mathcal{M}_A(f)) \subset \mathcal{Q}(A, C_S \circ \text{WF}(f))$. As with the PAT case, $\mathcal{Q}(A, C_S \circ \text{WF}(f))$ breaks into the union of three sets

$$\mathcal{Q}(A, C_S \circ \text{WF}(f)) = [C_S \circ \text{WF}(f) \cap \{(y, r), \eta) \in T^*(\Xi_S) : y \in K\}] \quad (57)$$

$$\cup \text{WF}(\chi_A) \cup W_A(f) \quad (58)$$

where

$$W_A(f) = \left\{ ((y, r), \eta \mathbf{d}y + \alpha [\mathbf{n}'(y, \tilde{x}) \mathbf{d}y + \mathbf{d}r]) : (y, \eta) \in N(K), \right. \\ \left. \alpha \neq 0, \tilde{x} \in S(y, r), \text{ and } (\tilde{x}, \alpha \mathbf{n}(y, \tilde{x}) \mathbf{d}x) \in \text{WF}(f) \right\} \quad (59)$$

corresponds to the sum of covectors $((y, r), \eta \mathbf{d}y) \in \text{WF}(\chi_A)$ and covectors

$$((y, r), \alpha [\mathbf{n}'(y, \tilde{x}) \mathbf{d}y + \mathbf{d}r]) \in \text{WF}(C_S \circ \text{WF}(f)).$$

We now examine the fibers of $W_A(f)$. Fix $r > 0$, and $\alpha_0 \neq 0$ and $(y, \eta_0) \in N(K)$. Assume there is a $\tilde{x} \in S(y, r)$ with $(\tilde{x}, \alpha_0 \mathbf{n}(y, \tilde{x}) \mathbf{d}x) \in \text{WF}(f)$. Note that

$$\forall a \neq 0, ((y, r), a \eta_0 \mathbf{d}y) \in \text{WF}(\chi_A), \quad \forall b > 0, ((y, r), b \alpha_0 [\mathbf{n}'(y, \tilde{x}) \mathbf{d}y + \mathbf{d}r]) \in C_S \circ \text{WF}(f). \quad (60)$$

The first statement in (60) follows because χ_A is a real valued function so a can be negative as well as positive (for real f and any real cutoff function φ , $\widehat{\varphi f}(\xi)$ is the complex conjugate of $\widehat{\varphi f}(-\xi)$). The right-hand statement in (60) is true since $\text{WF}(f)$ is conic. Therefore the part of the fiber of $W_A(f)$ above (y, r) that comes from a singularity of f at $(\tilde{x}, \alpha_0 \mathbf{n}(y, \tilde{x}))$ consists of points

$$((y, r), [a \eta_0 + b \alpha_0 \mathbf{n}'(y, \tilde{x})] \mathbf{d}y + b \alpha_0 \mathbf{d}r) \quad \text{for } a \in \mathbb{R}, b > 0. \quad (61)$$

At this point, we have finished steps (a) to (d) of the paradigm of Section 3.

The rest of the proof of (32) is similar to the proof of Theorem 4.2. Composing $\mathcal{Q}(A, C_S \circ \text{WF}(f))$ with C_S^t , one sees that $C_S^t \circ \mathcal{Q}(A, C_S \circ \text{WF}(f))$ is the union of three sets. The first set, from containment (57) becomes $C_S^t \circ [C_S \circ \text{WF}(f) \cap \{(y, r), \eta) \in T^*(\Xi_S) : y \in K\}] = \text{WF}(f) \cap \mathcal{V}_{S, K}$. The second composition is $C_S^t \circ \text{WF}(\chi_A) = \emptyset$ since c^{-1} is not defined unless the $\mathbf{d}r$ component is not zero. The third composition is $C_S^t \circ W_A(f)$ and this simplifies to $\mathcal{A}_{S, K}(f)$ if one uses (55) and the expression for part of the fiber of $W_A(f)$ given in (61).

Finally, one applies Lemma 3.2, (15) to finish the proof of (32).

To prove the second assertion in Theorem 4.6 if P is elliptic, we use the result of Theorem 4.8, (33), which is proven independently of this part of the proof. Let $(x, \xi \mathbf{d}\mathbf{x}) \in \text{WF}(f) \cap \mathcal{V}_{\mathcal{S}, \text{int}(K)}$ and let $y = y(x, \xi)$ be the point in $\text{int}(K)$ that is the center of the sphere $S(y(x, \xi), r(x, \xi))$ containing x and which is normal to ξ at x . Now, let φ be a cutoff function that is supported in $\text{int}(K)$ and is equal to one in a compact set $K' \subset \text{int}(K)$ chosen so $y \in \text{int}(K')$. Then, by Theorem 4.8, $(x, \xi \mathbf{d}\mathbf{x}) \in \text{WF}(\mathcal{L}_\varphi(f))$. However,

$$(x, \xi \mathbf{d}\mathbf{x}) \notin \text{WF}(\mathcal{M}_{\mathcal{S}}^* P(\chi_A - \varphi) \mathcal{M}_{\mathcal{S}}(f))$$

for the following reasons. First, $(\chi_A - \varphi)$ is zero near (y, r) for all r . Thus $P(\chi_A - \varphi) \mathcal{M}_{\mathcal{S}}(f)$ is smooth near y and so $\mathcal{M}_{\mathcal{S}}^* P(\chi_A - \varphi) \mathcal{M}_{\mathcal{S}}(f)$ is smooth near $c^{-1}((y, r), \nu \mathbf{d}\mathbf{y} + \alpha \mathbf{d}\mathbf{r})$ whenever $\nu/\alpha \in D$. However, for some choice of r, ν , and α , $((y, r), \nu \mathbf{d}\mathbf{y} + \alpha \mathbf{d}\mathbf{r}) = c(x, \xi \mathbf{d}\mathbf{x})$ and so $(x, \xi \mathbf{d}\mathbf{x}) = c^{-1}((y, r), \nu \mathbf{d}\mathbf{y} + \alpha \mathbf{d}\mathbf{r})$. Thus $\mathcal{M}_{\mathcal{S}}^* P(\chi_A - \varphi) \mathcal{M}_{\mathcal{S}}(f)$ is smooth near $(x, \xi \mathbf{d}\mathbf{x})$. These two results show that $(x, \xi \mathbf{d}\mathbf{x}) \in \text{WF}(\mathcal{M}_{\mathcal{S}}^* P \mathcal{M}_{\mathcal{S}, A}(f))$ and this proves the second part of the theorem. \square

Proof of Theorem 4.8. Let φ be a cutoff function supported in $\text{int}(K)$ and equal to one on the set K' given in the statement of this theorem. Then, \mathcal{K}_φ is trivially a pseudodifferential operator on $\mathcal{E}^*(\Xi_{\mathcal{S}})$ and so $PK_\varphi \mathcal{M}_{\mathcal{S}}$ is a FIO associated to $C_{\mathcal{S}}$. Now, by (56), \mathcal{L}_φ is a standard pseudodifferential operator, and this proves the first part of Theorem 4.8.

To prove the ellipticity statement, (33), let $(x, \xi \mathbf{d}\mathbf{x}) \in \text{WF}(f) \cap \mathcal{V}_{\mathcal{S}, K'}$ and assume P is elliptic. Let $\nu \in T_{(y, r)}^*(\Xi)$ and $((y, r), \nu) = c(x, \xi \mathbf{d}\mathbf{x})$. Because $(x, \xi \mathbf{d}\mathbf{x}) \in \mathcal{V}_{\mathcal{S}, K'}$, $y \in K'$. Because $\mathcal{M}_{\mathcal{S}}$ is elliptic (and $\Pi_L : C \rightarrow T^*(\Xi)$ is an injective immersion) and PK_φ is elliptic near $((y, r), \nu)$, one sees that $((y, r), \nu) \in \text{WF}(PK_\varphi \mathcal{M}_{\mathcal{S}}(f))$. Since $\mathcal{M}_{\mathcal{S}}^*$ is elliptic and both c and c^{-1} are functions, $c^{-1}((y, r), \nu) = (x, \xi \mathbf{d}\mathbf{x})$ and $(x, \xi \mathbf{d}\mathbf{x}) \in \text{WF}(\mathcal{L}_\varphi(f))$. This proves the second part of the theorem. \square

Remark A.1. In the case of sonar, we can assert, if P is elliptic, that $\mathcal{M}_{\mathcal{S}}^* PK_\varphi \mathcal{M}_A$ is elliptic on $\mathcal{V}_{\mathcal{S}, \text{int}(K')}$ because composition with $C_{\mathcal{S}}$ and $C_{\mathcal{S}}^t$ is described by two functions, c and c^{-1} . This reflects the fact that for each $(x, \xi \mathbf{d}\mathbf{x}) \in \mathcal{V}_{\mathcal{S}, \mathbb{R}^2}$ there is a unique $((y, r), \nu)$ in $C_{\mathcal{S}} \circ \{(x, \xi \mathbf{d}\mathbf{x})\}$. In the case of the circular transform in PAT, there are two such covectors, corresponding to the two angles $\phi_1(x, \xi)$ and $\phi_2(x, \xi)$ in the proof of Theorem 4.2. For the circular transform, to assert that $\mathcal{M}^* PK_\varphi \mathcal{M}$ is elliptic in $\mathcal{V}_{(a', b')}$, one would have to calculate the symbol of $\mathcal{M}^* PK_\varphi \mathcal{M}$ and make sure it is nowhere zero on $\mathcal{V}_{(a', b')}$.

This argument implies that $\mathcal{M}^* \mathcal{K}_\varphi \mathcal{M}$ is elliptic on $\mathcal{V}_{(a', b')}$ since the symbol consists of terms that are positive above $\mathcal{V}_{(a', b')}$ (see e.g., [12, 13, 32]). The same argument shows that $\mathcal{M}^* P \mathcal{M}$ would be elliptic on $\mathcal{V}_{(a', b')}$ when P is a pseudodifferential operator with top-order symbol that is everywhere positive (or everywhere negative) above $(a', b') \times (0, \infty)$.

As a simple example where this is not true, if R is the Radon line transform and R^* is its dual, then $R^*(d/dp)R = 0$ even though each operator is elliptic (d/dp is elliptic on $\text{range}(R)$).

Remark A.2. Our analysis is simplified because $C^t \circ C \subset \Delta$ in (49) and (56). Because of this, the set of “visible” singularities ((46) for PAT and $C_{\mathcal{S}}^t$ composed with the first set in (57) for sonar) is a subset of $\text{WF}(f)$ since $C^t \circ (C \circ \text{WF}(f)) \subset \Delta \circ \text{WF}(f) = \text{WF}(f)$.

If C is the canonical relation of a FIO \mathcal{F} and $\Pi_L : C \rightarrow T^*(\Xi)$ is an injective immersion, then $C^t \circ C \subset \Delta$ and if they can be composed, $\mathcal{F}^* \mathcal{F}$ is a pseudodifferential operator [12, 13, 32].

When $C^t \circ C$ is not a subset of Δ , singularities can be added by the backprojection itself, even with a smooth cutoff in place of χ_A . This comes up, for example, in common midpoint synthetic aperture radar: the normal operator $\mathcal{M}^* \mathcal{M}$ is not even a FIO but a sum of singular FIOs associated with different canonical relations [2].

- [1] M. AGRANOVSKY AND E. T. QUINTO, *Injectivity sets for Radon transform over circles and complete systems of radial functions*, J. Functional Anal., 139 (1996), pp. 383–414.
- [2] G. AMBARTSOUMIAN, R. FELEA, V. KRISHNAN, C. NOLAN, AND E. T. QUINTO, *A class of singular Fourier integral operators in synthetic aperture radar imaging*, Journal of Functional Analysis, 264 (2013), pp. 246–269.
- [3] L.-E. ANDERSSON, *On the determination of a function from spherical averages*, SIAM J. Math. Anal., 19 (1988), pp. 214–232.
- [4] A. BUEHLER, A. ROSENTHAL, T. JETZFELLNER, A. DIMA, D. RAZANSKY, AND V. NTZIACHRISTOS, *Model-based optoacoustic inversions with incomplete projection data*, Medical Physics, 38 (2011), p. 1694.
- [5] J. COHEN AND N. BLEISTEIN, *Velocity inversion procedure for acoustic waves*, Geophysics, 44 (1979), pp. 1077–1085.
- [6] P. ELBAU, O. SCHERZER, AND R. SCHULZE, *Reconstruction formulas for photoacoustic sectional imaging*, Inverse Problems, 28 (2012), p. 045004.
- [7] A. FARIDANI, D. FINCH, E. L. RITMAN, AND K. T. SMITH, *Local tomography, II*, SIAM J. Appl. Math., 57 (1997), pp. 1095–1127.
- [8] A. FARIDANI, E. L. RITMAN, AND K. T. SMITH, *Local tomography*, SIAM J. Appl. Math., 52 (1992), pp. 459–484.
- [9] D. FINCH, S. PATCH, AND RAKESH, *Determining a function from its mean values over a family of spheres*, SIAM J. Math. Anal., 35 (2004), pp. 1213–1240.
- [10] F. G. FRIEDLANDER, *Introduction to the theory of distributions*, Cambridge University Press, Cambridge, second ed., 1998. With additional material by M. Joshi.
- [11] J. FRIKEL AND E. T. QUINTO, *Characterization and reduction of artifacts in limited angle tomography*, Inverse Problems, 29 (2013), p. 125007.
- [12] V. GUILLEMIN, *Some remarks on integral geometry*, tech. rep., MIT, 1975.
- [13] V. GUILLEMIN AND S. STERNBERG, *Geometric Asymptotics*, American Mathematical Society, Providence, RI, 1977.
- [14] M. HALTMEIER, O. SCHERZER, AND G. ZANGERL, *A Reconstruction Algorithm for Photoacoustic Imaging Based on the Nonuniform FFT*, IEEE Transactions on medical imaging, 28 (2009), pp. 1727–1735.
- [15] M. HALTMEIER, T. SCHUSTER, AND O. SCHERZER, *Filtered backprojection for thermoacoustic computed tomography in spherical geometry*, Mathematical Methods in the Applied Sciences, 28 (2005), pp. 1919–1937.
- [16] L. HÖRMANDER, *Fourier Integral Operators, I*, Acta Mathematica, 127 (1971), pp. 79–183.
- [17] L. HÖRMANDER, *The analysis of linear partial differential operators. I*, Classics in Mathematics, Springer-Verlag, Berlin, 2003. Distribution theory and Fourier analysis, Reprint of the second (1990) edition [Springer, Berlin].
- [18] M. JAEGER, S. SCHÜPBACH, A. GERTSCH, M. KITZ, AND M. FRENZ, *Fourier reconstruction in optoacoustic imaging using truncated regularized inverse k -space interpolation*, Inverse Problems, 23 (2007), pp. S51–S63.

- [19] A. KATSEVICH, *Local tomography for the limited-angle problem*, J. Math. Anal. Appl., 213 (1997), pp. 160–182.
- [20] P. KUCHMENT AND L. KUNYANSKY, *Mathematics of photoacoustic and thermoacoustic tomography*, in Handbook of Mathematical Methods in Imaging, O. Scherzer, ed., Springer, 2010, pp. 817–866.
- [21] L. KUNYANSKY, *Explicit inversion formulas for the spherical mean Radon transform*, Inverse Problems, 23 (2007), pp. 373–383.
- [22] G. LAURITSCH AND H. BRUDER, *FORBILD head phantom*. <http://www.imp.uni-erlangen.de/phantoms/head/head.html>.
- [23] F. NATTERER, *The mathematics of computerized tomography*, B. G. Teubner, Stuttgart, 1986.
- [24] L. V. NGUYEN, *On a reconstruction formula for spherical Radon transform: a microlocal analytic point of view*, Analysis and Mathematical Physics, (2013), pp. 1–22.
- [25] ———, *How strong are streak artifacts in limited angle tomography*, tech. rep., University of Idaho, 2014.
- [26] L. V. NGUYEN, *On Artifacts in Limited Data Spherical Radon Transform I: Flat Observation Surfaces*, arXiv:1407.4496 [math.CA], (2014).
- [27] C. J. NOLAN AND M. CHENEY, *Synthetic Aperture inversion*, Inverse Problems, 18 (2002), pp. 221–235.
- [28] V. PALAMODOV, *Reconstruction from Limited Data of Arc Means*, J. Fourier Analysis and Applications, 6 (2000), pp. 25–42.
- [29] H. S. PARK, J. K. CHOI, AND J. K. SEO, *Characterization of Metal Artifacts in X-ray Computed Tomography*, tech. rep., Yonsei University, Korea, 2014.
- [30] I. PATRICKEYEV AND A. A. ORAEVSKY, *Removing image artifacts in optoacoustic tomography using virtual transducer restoration*, Proc. SPIE, 5320 (2004), pp. 249–256.
- [31] B. PETERSEN, *Introduction to the Fourier Transform and Pseudo-Differential Operators*, Pittman, Boston, 1983.
- [32] E. T. QUINTO, *The dependence of the generalized Radon transform on defining measures*, Trans. Amer. Math. Soc., 257 (1980), pp. 331–346.
- [33] E. T. QUINTO, *Singularities of the X-ray transform and limited data tomography in \mathbb{R}^2 and \mathbb{R}^3* , SIAM J. Math. Anal., 24 (1993), pp. 1215–1225.
- [34] E. T. QUINTO, A. RIEDER, AND T. SCHUSTER, *Local inversion of the sonar transform regularized by the approximate inverse*, Inverse Problems, 27 (2011), p. 035006 (18p).
- [35] D. RAZANSKY, M. DISTEL, C. VINEGONI, R. MA, N. PERRIMON, R. W. KÖSTER, AND V. NTZACHRISTOS, *Multispectral opto-acoustic tomography of deep-seated fluorescent proteins in vivo*, Nature Photonics, 3 (2009), pp. 412–417.
- [36] W. RUDIN, *Functional analysis*, McGraw-Hill Book Co., New York, 1973. McGraw-Hill Series in Higher Mathematics.
- [37] W. SYMES, *Mathematics of Reflection Seismology*, tech. rep., Rice University, 1998.
- [38] F. TRÈVES, *Introduction to Pseudodifferential and Fourier Integral Operators*, Volume 2: Fourier Integral Operators, Plenum Press, New York and London, 1980.
- [39] Y. XU, L. V. WANG, G. AMBARTSOUMIAN, AND P. KUCHMENT, *Reconstructions in limited-view thermoacoustic tomography*, Medical Physics, 34 (2004), pp. 724–733.